Advances in Geo-Energy Research

Vol. 17, No. 3, p. 212-225, 2025

Original article

Evolution of microstructural damage in coal under supercritical CO_2-water exposure: A multi-scale study incorporating the indentation size effect

Bozhi Deng[1], Bingyang Jiao[1], Baisheng Nie[1]*, Changbao Jiang[1]*, Minghui Li[2,3], Yumeng Zhao[4]

[1]*State Key Laboratory of Coal Mine Disaster Dynamics and Control, Chongqing University, Chongqing 400030, P. R. China*

[2]*State Key Laboratory of Intelligent Construction and Healthy Operation and Maintenance of Deep Underground Engineering, Shenzhen University, Shenzhen 518060, P. R. China*

[3]*Guangdong Provincial Key Laboratory of Deep Earth Sciences and Geothermal Energy Exploitation and Utilization, Shenzhen University, Shenzhen 518060, P. R. China*

[4]*Department of Civil and Environmental Engineering, University of Nebraska-Lincoln, Omaha 68106, USA*

Keywords:

CO_2-water-coal interaction
nanoindentation
erosion quantification
indentation size effect
micromechanical properties

Cited as:

Deng, B., Jiao, B., Nie, B., Jiang, C., Li, M., Zhao, Y. Evolution of microstructural damage in coal under supercritical CO_2-water exposure: A multi-scale study incorporating the indentation size effect. Advances in Geo-Energy Research, 2025, 17(3): 212-225.
https://doi.org/10.46690/ager.2025.09.04

Abstract:

CO_2 sequestration in coal seams represents an effective strategy for mitigating CO_2 emissions. However, the complicated interaction of CO_2-water-coal at the micro-scale may compromise the structural integrity and mechanical strength of coal, thereby adversely impacting the efficacy and safety of CO_2 sequestration in coal seams. This study introduces a novel indentation testing method that reveals the scale-dependent evolution mechanisms of coal microstructures, enabling the accurate and reliable quantification level of degradation in the micromechanical properties caused by supercritical CO_2-water-coal interactions. Using this method, the extent of mechanical degradation in three types of coal microstructures could be accurately evaluated under supercritical CO_2-water-coal interaction. The pure organic matrix exhibited remarkable stability under all fluid treatments, with minor changes in microstructure feature and a mechanical property reduction of less than 25%. In contrast, the mineral structures were significantly altered by treatment with fluid mixed with supercritical CO_2 and brine, with erosion depths and mechanical property reductions reaching 1.6 μm and 80% in granular structures, and 6.4 μm and 90% in banded structures. However, in the absence of brine or supercritical CO_2, the erosion depths and mechanical property reductions of fusinite were limited.

1. Introduction

In 2024, global energy-related carbon dioxide (CO_2) emissions exceeded 37.8 billion metric tons. Among these, Chinese carbon emissions reached 12.6 billion metric tons, solidifying its position as the world's largest emitter (Friedlingstein et al., 2025). These substantial CO_2 emissions significantly exacerbate climate challenges, such as global warming and the rising frequency of extreme weather events. As a result, implementing sustainable action to reduce atmospheric CO_2 levels is essential to mitigate the global greenhouse effect and prevent its far-reaching consequences.

By 2070, CO_2 geological storage technology is expected to contribute 15% of cumulative emission reductions in the global energy sector, making it a crucial strategy for deep CO_2 emission reduction. Currently, numerous unmineable coal seams provide suitable target reservoirs for CO_2 geological storage (Fender et al., 2020; Safaei-Farouji et al., 2025). When

Yandy Scientific Press

*Corresponding author.
E-mail address: dengbz@cqu.edu.cn (B. Deng); jiaoby@stu.cqu.edu.cn (B. Jiao); bshnie@cqu.edu.cn (B. Nie); JCB@cqu.edu.cn (C. Jiang); mhli@szu.edu.cn (M. Li); yzhao52@unl.edu (Y. Zhao).

Received July 10, 2025; revised August 5, 2025; accepted August 23, 2025; available online August 27, 2025.

the depth of target coal seams surpasses 800 m, CO_2 is typically stored in reservoirs in a supercritical state (Jiang and Yu, 2019; Liu et al., 2023b; Shen et al., 2024). Supercritical CO_2 ($ScCO_2$) interacts with coal and brine, altering the reservoir's physical and chemical properties, and such interaction may increase the risk of CO_2 leakage from geological formations (Sampath et al., 2019; Chen et al., 2023). Therefore, quantifying the extent of $ScCO_2$-water-coal interaction and investigating the resulting evolution of the mechanical properties of coal are essential for evaluating the safety and feasibility of CO_2 sequestration in unmineable coal seams (Zhang et al., 2022a; Bashir et al., 2024).

The acidic environment formed when $ScCO_2$ dissolves in groundwater or brine can promote the dissolution of minerals, thereby altering the pore structure and mechanical properties of coal (Siqueira et al., 2017; Meng and Qiu, 2018; Zagorščak and Thomas, 2018; Su et al., 2023). Studies have shown that the mineral composition of coal changes significantly under the $ScCO_2$-water-coal interaction. While some minerals represented by carbonates dissolve, secondary minerals such as gypsum are also formed (Jiang and Yu, 2019; Zhang et al., 2023). Furthermore, the influence of $ScCO_2$-water-coal interaction also leads to a slight increase in the coal micropore volume, indicating that the dissolution of some minerals caused by $ScCO_2$-water-coal interaction changes the coal's pore structure (Liu et al., 2019; Xu et al., 2022). On the other hand, the mechanical properties of coal also decrease to different degrees before and after the $ScCO_2$-water-coal interaction, which may be related to the water content (Zhou et al., 2024) and CO_2 phase state (Perera et al., 2013) during the reaction process. These studies establish that the $ScCO_2$-water-coal interaction can alter the compositions, structures and mechanical properties of coal. However, they fail to decipher the underlying mechanisms, which presents opportunities for further in-depth research.

The $ScCO_2$-water-coal interaction occurs at the micro-scale, and the macroscopic changes in coal properties are the cumulative result of numerous micro-scale interactions (Gathitu et al., 2009; Niu et al., 2024; Mouallem et al., 2025). Under laboratory conditions with limited treatment durations, the impact of this interaction on the macroscopic mechanical properties of coal is insignificant. Therefore, many researchers have turned to advanced techniques such as X-ray diffraction and scanning electron microscopy (SEM) to characterize the effects of the $ScCO_2$-water-coal interaction on the mineral composition and microscopic surface topography of coal. At the microscopic scale, the injection of $ScCO_2$ significantly increases the pore volume and porosity of coal, while the content of carbonate minerals in coal decreases notably (Chen et al., 2022). Observations via SEM reveal that the formation of new pores on the coal surface after $ScCO_2$-water-coal interaction is mainly caused by the dissolution of carbonate minerals, whereas no obvious dissolution of silicate minerals occurs (Masoudian et al., 2014). Therefore, the dissolution of carbonate minerals is the key factor contributing to the changes in the pore structure and surface topography of coal induced by the $ScCO_2$-water-coal interaction.

Nanoindentation is a micro-scale technology that is especially popular for rock characterization, which excels in quantifying variations in the mechanical properties such as the hardness and elastic modulus of composite materials at the nano- and micro-scales. Studies have consistently demonstrated such micromechanical heterogeneity in coals (Zhang et al., 2018; Kossovich et al., 2020; Liu and Liu, 2022; Kossovich et al., 2023). Nanoindentation is also widely used to examine fluid-rock matrix interactions, as alterations in surface topography and physical properties can be induced within a short period and readily measured at the nanoscale (Manjunath et al., 2023). In contrast, larger-scale tests would require prohibitively long interaction times to capture such phenomena. Reports show that CO_2-water treatment significantly weakens coal, manifested as drops in hardness and Young's modulus caused primarily by the dissolution of carbonate minerals (Liu et al., 2023a; He et al., 2024). Such reduction has also been verified by comparative micro-imaging analyses (Liu and Liu, 2022; Zhang et al., 2022b). All of the aforementioned studies focused on statistically analyzing nanoindentation on CO_2-water altered coals under a single loading condition, which is insufficient for quantifying erosion depth. On the other hand, the continuous multi-cycle loading method fills the gap and provides valuable information on the effect of $ScCO_2$-water-coal interaction as the weakening layer deepens over time.

Although numerous studies on the $ScCO_2$-water-coal interaction have focused on the dissolution of coal mineral components, alterations in pore structure, and the weakening of micromechanical properties, few have comprehensively quantified erosion depth from the perspective of surface topography and changes in the mechanical properties among different coal microstructures induced by the $ScCO_2$-water-coal interaction. Therefore, this study employed SEM, three-dimensional (3D) laser confocal microscopy and nanoindentation to investigate the damage of coal microstructures under fluid treatment. The use of this novel indentation loading method provides a reliable basis for quantifying the weakening of micromechanical properties. By analyzing the changes in the mechanical properties and surface topography of coal microstructures, the interaction of $ScCO_2$-water-coal was quantitatively characterized at the micro-scale. Furthermore, the effects of treatment fluid (pure $ScCO_2$, brine, and $ScCO_2$-brine) and coal microstructures on the degree of mineral erosion were systematically analyzed. The findings provide valuable references for reservoir selection and safety evaluation in CO_2 sequestration within unmineable coal seams.

2. Materials and methods

2.1 Sample and brine preparation

The coal samples used in the experiments were collected from Baijiao Coal Mine in Gongxian County, Yibin City, Sichuan Province, and processed into 20 mm × 20 mm × 20 mm cubic shapes using wire cutting equipment. To meet the requirements of indentation experiments, the surface of the resulting specimens was sequentially polished using 600, 1,200, 2,000 and 5,000 mesh sandpaper (Fig. 1). To align with the actual geological conditions, the brine used in this exper-

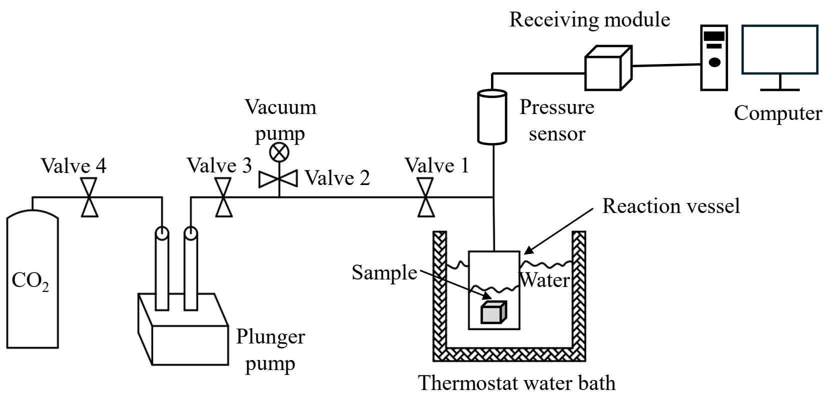

Fig. 1. $ScCO_2$-water-coal interaction device.

Table 1. Ionic concentrations of 1 L brine used in the experiment.

Ion	Concentration (mg/L)
Ca^{2+}	198.5
Mg^{2+}	18.26
$SO_4{}^{2-}$	240.2
$HCO_3{}^{-}$	438.8

Table 2. Experimental scheme for soaking.

Soaking fluid	Temperature (°C)	Pressure (MPa)	Time (d)
Brine	40	0	10
$ScCO_2$	40	8	10
$ScCO_2$-brine	40	8	10

iment was prepared based on the water quality test results from Baijiao Coal Mine, with $CaCl_2$ at 555 mg/L, $MgCl_2 \cdot 6H_2O$ at 169.2 mg/L, $NaHCO_3{}^-$ at 619.7 mg/L, and Na_2SO_4 at 340.2 mg/L. Meanwhile, the ion concentrations of the prepared brine was detected (Table 1).

2.2 Experimental procedures

(1) Scanning electron microscope-energy dispersive spectroscopy analysis

A TM4000 Plus bench-top scanning electron microscope (SEM) with energy-dispersive X-ray spectroscopy (EDS) spectroscopy was used to observe the microstructures on the surface of rock samples at 500× magnification before soaking treatment. EDS spectroscopy was also performed to analyze the components.

(2) High-temperature and high-pressure soaking

To investigate the characteristics of the complex $ScCO_2$-water-coal interaction, three forms of fluid soaking conditions were established: $ScCO_2$ soak, brine soak, and $ScCO_2$-brine soak (Table 2, Fig. 1). The soak temperature was set at 40 °C, and the CO_2 pressure was maintained at 8 MPa to ensure that CO_2 reached a supercritical state. To ensure a full interaction of the samples, the soaking time was set at 10 days.

(3) Observation of surface erosion and quantification of erosion depth

To analyze the microstructural damage on the coal surface before and after soaking in different fluids, laser scanning was performed using a LEXT OLS 4000 laser confocal microscope. The observations focused on the surface of coal samples before and after the treatments, with particular attention to damage variations in the filler regions.

The scanning results (1,024 × 1,024-pixel coordinate data, 256 μm × 256 μm) were processed using MATLAB to generate two-dimensional (2D) cloud maps of the regions. To further quantify the extent of fluid erosion on different components of the coal sample surface, the 1,024 × 1,024 points coordinate matrix was divided into 32 × 32 smaller matrices, each comprising 32 × 32 points. The root-mean-square deviation (RMSD) was calculated to quantify the degree of erosion within each matrix. Subsequently, an RMSD map was plotted, and the average height of the points within each smaller matrix was calculated as the matrix height. When the RMSD of smaller matrices were greater than that of the microstructural surface before soaking, the smaller matrices were considered to have been affected by erosion. Conversely, when the RMSD of smaller matrices were less than or equal to that of the microstructural surface before soaking, the smaller matrices were deemed unaffected by erosion. For the specific calculation method, please refer to Appendix A of the Supplementary file.

(4) Indentation experiments in continuous multi-cycle loading mode

This experiment utilized the Nanotest Alpha testing equipment, capable of delivering a maximum load of 500 mN with a load resolution of 3 nN. This apparatus provides a broad testing range and high precision, fully satisfying the experimental requirements.

The indentation test in continuous multi-cycle (CMC) loading mode was performed using the progressive loading/unloading method, allowing multiple cycles with varying loads at the same location. This approach offers the advantage of monitoring the changes in mechanical properties, including hardness and elasticity modulus, as a function of indentation

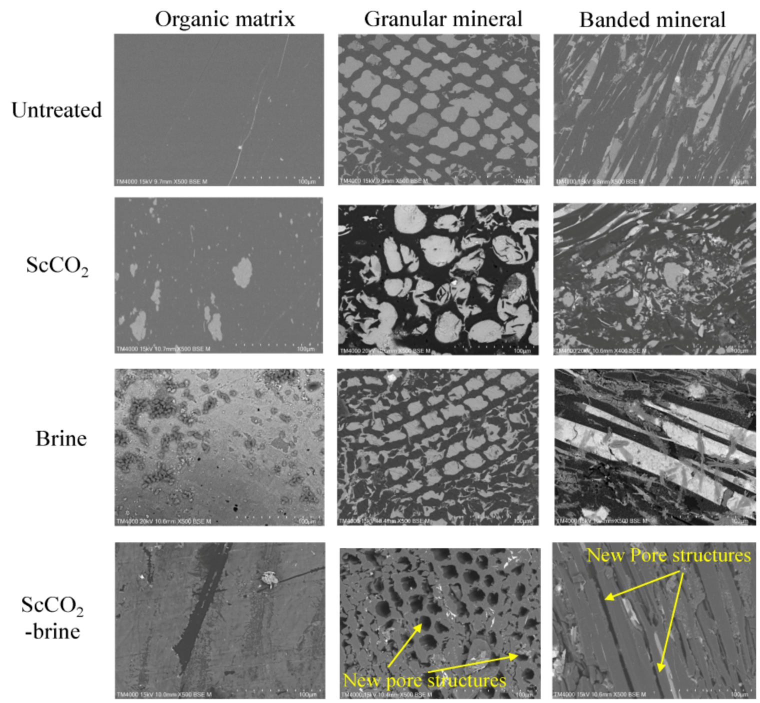

Fig. 2. Changes in the surface topography of the three microstructures in coal samples under different fluid treatments (observed using SEM).

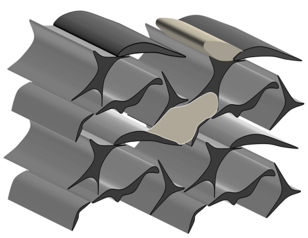

Fig. 3. 3D sketch of a typical mineral structure in fusinite.

depth. The multi-scale micromechanical properties obtained via this loading method facilitate the cross-scale quantification of erosion degree induced by the $ScCO_2$-brine-coal interaction.

The CMC loading mode indentation experiment employs the Oliver and Pharr analysis method, akin to the standard mode indentation experiment, to calculate the mechanical properties during a single loading/unloading cycle. This strategy facilitates the determination of mechanical properties at each load in the CMC loading mode.

In this experiment, nanoindentation tests in the CMC loading mode were performed using a Berkovich indenter on coal samples. The samples underwent four treatment conditions: Untreated, brine soaking, $ScCO_2$ soaking, and $ScCO_2$ + brine soaking. A 3 × 3 grid layout of indentation tests was set across three distinct regions of the coal samples: Granular mineral structure, filamentous mineral structure, and organic matrices structure. The distance between each indentation point was set at 100 μm to ensure their independence. Ten distinct peak loads were established at regular intervals within the range of 0.5 to 480 mN, with the peak loads of 0.5 and 480 mN designated for the initial and final cycles, respectively. During each cycle, the indenter was loaded to the specified value at a rate of 8 mN/s, and the load-holding process lasted for 40 seconds. This was followed by unloading of the indenter at a rate of 8 mN/s to 20% of the peak load in that cycle, after which the indenter proceeded to the next cycle. Upon completion of the final cycle, the load was fully unloaded to zero.

(5) Calculation of mechanical parameters (modulus and hardness)

The classical mechanical parametric analysis method, proposed by Oliver and Pharr, focuses on analyzing and calculating the measured continuous load and displacement variation data (Joslin and Oliver, 1990). Through this process, the load-displacement curve (known as the *P*-*h* curve) was first obtained, and then the hardness and elastic modulus of the coal surface were determined. For the specific calculation method, please refer to Appendix B of the Supplementary file.

3. Results

3.1 Observation of coal microstructures

3.1.1 Typical components and microstructures

As is well-known, coal consists of organic matrices and various minerals. Organic matrices are the predominant components, incorporating various mineral fillings and forming diverse organic matter-mineral structures at the micro-scale. In our previous studies (Deng et al., 2022; Jiang et al., 2025), we provided a comprehensive analysis of the typical mineral types and structures observed in coal. Using SEM, the organic matrix of vitrinite and the mineral structures of fusinite on coal were observed (Fig. 2). In fusinite, the mineral structures are filled in the 3D scan (Fig. 3), resulting in anisotropy on the

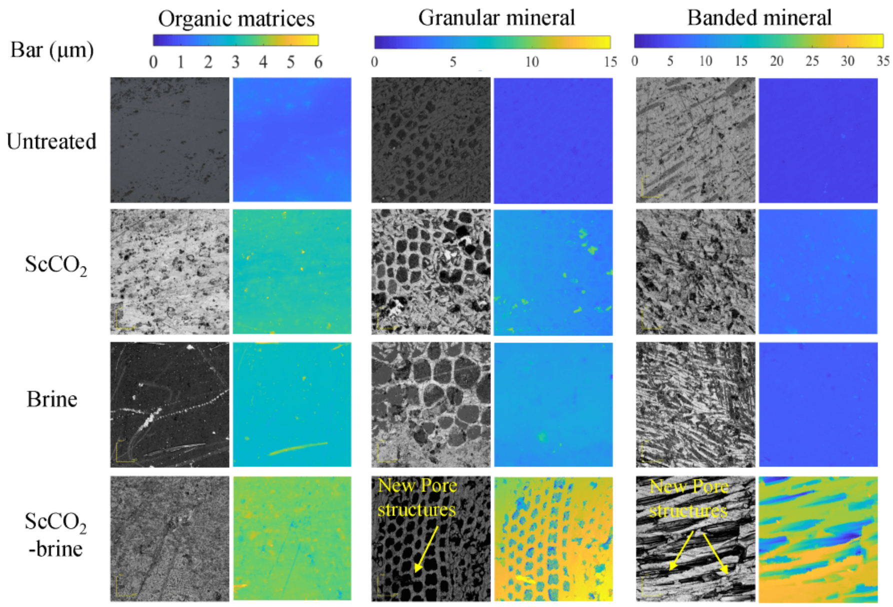

Fig. 4. Changes in the surface topography of the three microstructures in coal samples under different fluid treatments (observed using 3D laser scanning).

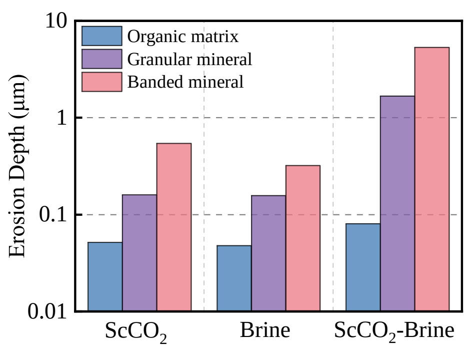

Fig. 5. Erosion depth.

2D scan. Moreover, EDS analysis of the observed areas further revealed that carbonate and quartz minerals are the principal components filling the mineral microstructures and organic matrices in fusinite and vitrinite, respectively. The surface mineral structures of the Baijiao coal sample are mainly characterized by granular mineral and banded mineral formations in the 2D scan.

3.1.2 Surface erosion

The surface topography changes were observed in the three microstructures following soaking in various treatment fluids (Fig. 2). SEM analysis revealed that the extent of surface modification is influenced by both the treating fluid type and the coal microstructure. Organic matrices exhibited minimal surface topography changes after fluid exposure, with no significant erosion pits detected. In contrast, both mineral microstructure types exhibited noticeable surface alterations, with a partial dissolution of surface minerals observed after treatment with $ScCO_2$ and brine. The most pronounced topological changes occurred in filamentous mineral structures subjected to $ScCO_2$ + brine treatment, where the extensive dissolution of carbonate minerals resulted in the formation of substantial surface pits.

Using 3D laser scanning, changes in the surface topologies of coal samples can be quantitatively characterized by erosion depth. The surfaces of microstructures exposed to different treating fluids were submitted to 3D scanned by a laser confocal microscope. The surface height differences of the pure organic matrices were around 2 μm after soaking in different fluids (Fig. 4). For the granular and filamentous mineral structures, there was no significant change in surface height difference after soaking in pure $ScCO_2$ or brine. However, after soaking in $ScCO_2$ + brine, the surface height difference of these structures reached 10 and 15 μm, respectively.

The RMSD map is an effective tool for discerning the surface topographic characteristics of microstructures (Fig. 5). The RMSD of regions exhibiting pronounced erosion was markedly larger, whereas the RMSD of regions with minimal or no erosion was considerably smaller. The erosion depth of the organic matrix under the action of different fluids was calculated to be less than 0.1 μm, indicating that organic matter remains stable under treatment with all fluids. When exposed to $ScCO_2$ and brine, the erosion depths of two mineral structures were comparable (within 0.5 μm). However, the mineral structures exhibited significant and substantial erosion under $ScCO_2$-brine, with depths reaching 1.6 μm in granular structures and 6.4 μm in banded structures.

3.2 Continuous multi-cycle nanoindentation

3.2.1 Force-displacement curves

In order to investigate the changes in the micromechanical properties of each microstructure on the coal surface before and after treatment with different fluids, the Nanotest Alpha testing equipment was used to measure the changes in the mechanical properties of the pure organic matrix,

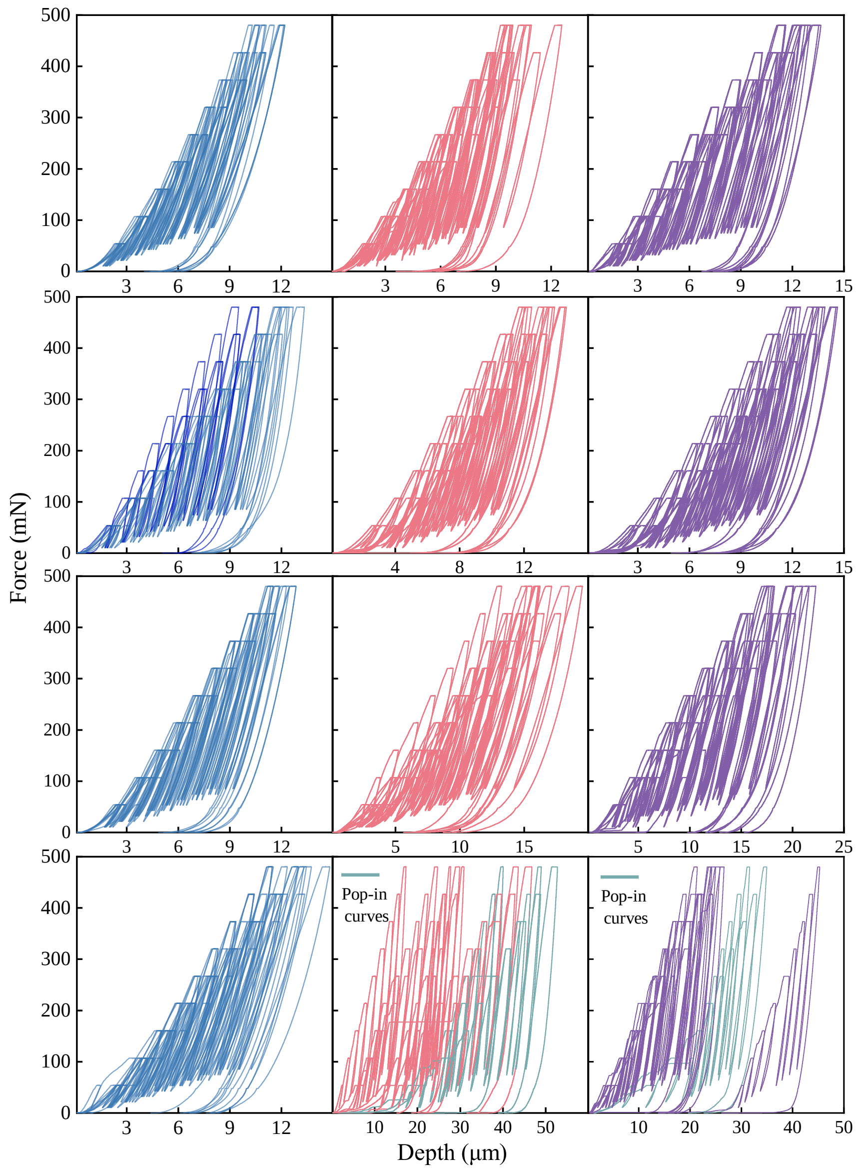

Fig. 6. Load-displacement curves of indentation test on different coal microstructures before/after treatment with different fluids.

granular mineral structures, and filamentous mineral structures under soaking in different fluids (pure $ScCO_2$, brine, and $ScCO_2$-brine). The corresponding force-displacement curves (F-h curves) of CMC loading nanoindentation experiments on organic matrices and mineral structures were presented. It is worth noting that the limitations of current observation technology result in the inclusion of mineral structures in the indentation region of the organic matrices after $ScCO_2$ treatment (Fig. 6), which could introduce anomalies into the dataset (the dark blue curves in organic matrices under $ScCO_2$ treatment). It was found that the indentation curves of the organic matrices before and after soaking treatments exhibited notable similarities. In contrast, the indentation curves of mineral structures exposed to $ScCO_2$ or brine soaking treatment demonstrated increased dispersion. Notably, mineral structures underwent the most significant alteration when submitted to $ScCO_2$ + brine treatment.

3.2.2 Changes in the mechanical parameters

Using the formula introduced in Section 2.2, the elasticity modulus and hardness of each microstructure under experimental conditions were calculated for each loading and unloading cycle. It is worth noting that the loading force of the first cycle was 0.5 mN, which is relatively small and closed to the accuracy limit of the equipment, potentially leading to significant errors in the mechanical parameter calculations. Therefore, only the last nine cycles were considered for analyzing the changes in the mechanical properties of coal microstructures, and a statistical analysis of the mechanical parameters was conducted (Fig. 7).

The variation in elastic modulus and hardness with increasing loading force for each microstructure before and after different fluid treatments was evident in that the mechanical parameters of untreated mineral structures were higher than

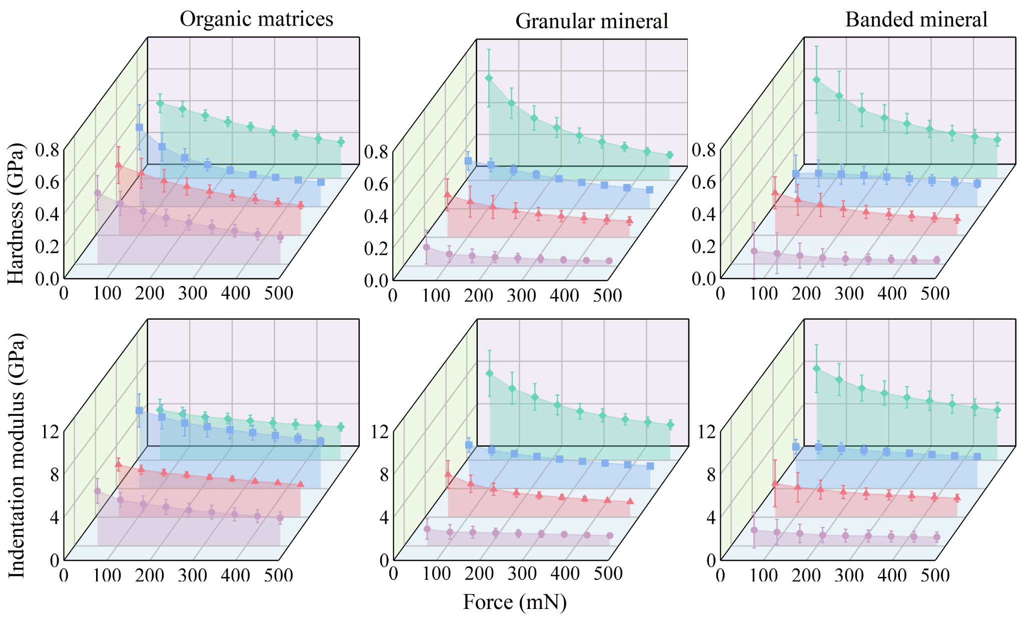

Fig. 7. Statistical analysis of the elastic modulus and hardness in each coal microstructure at different loading stages before/after treatment with different fluids.

those of the organic matrix. This is primarily due to the presence of numerous mineral fillings, which have stronger mechanical properties compared to organic matters (Fig. 7). However, after treatment with various fluids, the mechanical properties of the mineral structures decreased significantly. Notably, for mineral structures subjected to $ScCO_2$ + brine soaking, their mechanical parameters fell below those of the organic matrix, which may be attributed to the formation of new pore structures (Figs. 2 and 4) resulting from mineral dissolution.

Moreover, both mineral fillings and dissolution-induced hollow pores contribute to the increased heterogeneity of mineral structures. This led to a more scattered distribution and a higher standard deviation (Fig. 7) of the mechanical parameters in mineral structures compared to the organic matrix, which primarily consists of organic matters. At low loading forces, the indenter may interact individually with organic matters (the weaker component), minerals (the stronger component), or hollow pores. However, as the loading force increases, the indenter's contact area expands, gradually encompassing both strong and weak components within the mineral structure. This results in the convergence of the mechanical parameters, ultimately reflecting the composite mechanical properties of the mineral and organic components, a phenomenon known as Indentation Size Effect (ISE), which will be discussed in detail in Section 4.2.1.

4. Discussion

4.1 Extent of $ScCO_2$-water-coal interaction

4.1.1 Mechanism

The erosion depths of mineral structures were relatively minor. The partial dissolution of carbonates in the mineral structures and the height difference formed by the expansion of organic matters around the mineral structures (due to water absorption or CO_2 adsorption) were the most likely reasons for the slight erosion of the mineral structure when treated by $ScCO_2$ or brine (Shi et al., 2023). However, the $ScCO_2$-brine treatment resulted in the dissolution of a considerable number of calcite-based carbonate minerals due to the formation of an acidic solution from CO_2 and H_2O. This led to a pronounced erosion effect, with a significantly increased depth of erosion compared to the other two treatments.

Eqs. (1)-(3) depict the chemical interaction occurring in some minerals (Armitage et al., 2013; Wu and Zhu, 2025).

$$CO_2 + H_2O \leftrightarrows H^+ + CO_3{}^- \tag{1}$$

$$CaCO_3 + H^+ \leftrightarrows Ca^{2+} + H_2O + CO_2 \tag{2}$$

$$CaMg(CO_3)_2 + H^+ \leftrightarrows H_2O + CO_2 + Ca^{2+} + Mg^{2+} \tag{3}$$

Conversely, a significant discrepancy in erosion depth was observed between the granular and filamentous mineral structure areas subjected to $ScCO_2$-brine soaking treatment. The experimental results demonstrated that the erosion depth of the filamentous mineral structure area was significantly greater than that of the granular mineral structure area, which is attributed to the larger contact area of the banded mineral structure compared to the granular mineral structure (Sundal and Hellevang, 2019).

4.1.2 Mineral dissolution manifested in indentation

The indentation force-displacement curves of the two mineral structures under $ScCO_2$-brine treatment exhibited pronounced pop-in phenomena (Fig. 8) (Nie et al., 2024). This phenomenon refers to the brittle failure of microstructures within the coal samples during the loading process, characterized by a sudden increase in displacement and, in some

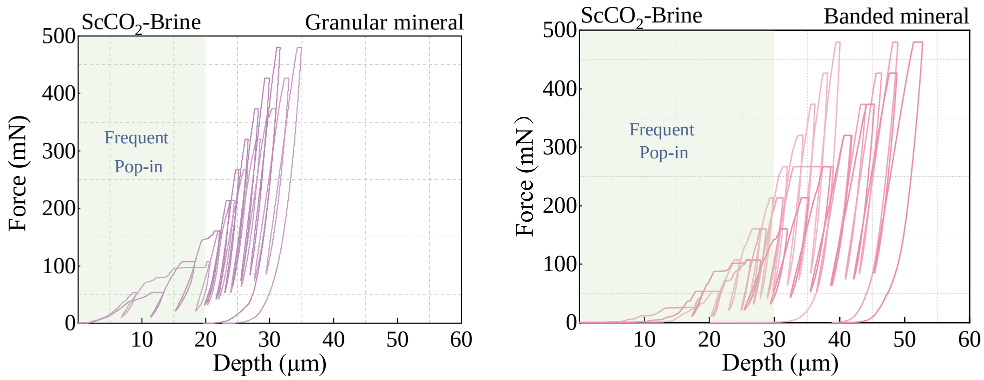

Fig. 8. Scope of the occurrence of pop-in events in the load-displacement curves of mineral structures under $ScCO_2$ + brine treatment.

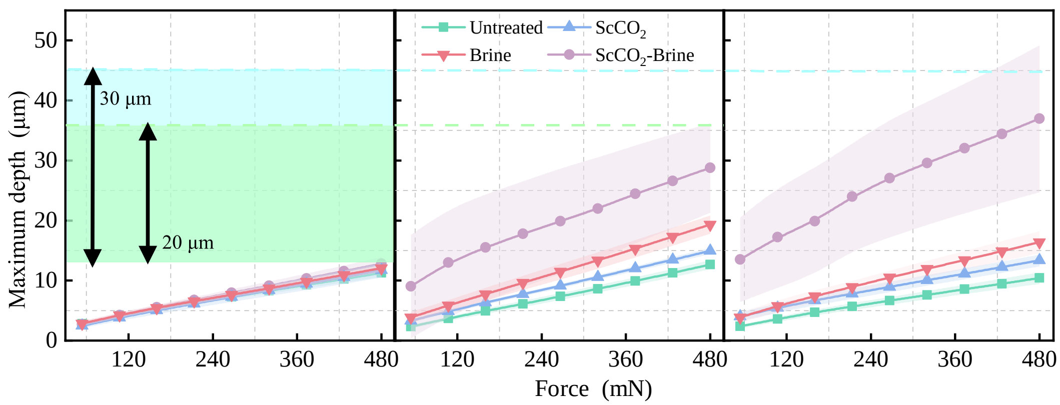

Fig. 9. Evolution of maximum indentation depth in each coal microstructure at different loading stages before/after treatment with different fluids.

cases, a slight decrease in loading force. In $ScCO_2$-water-coal interaction, the dissolution of carbonate minerals such as calcite and dolomite can lead to the formation of new pore structures (Figs. 2 and 4 under the condition of $ScCO_2$ + brine treatment). The failure of pore structures may trigger the pop-in phenomenon. However, when the indentation depth surpasses the mineral erosion depth, the force-displacement curves become continuous. Therefore, the depth at which pop-in events occur can indicate the erosion depth.

The force-displacement curves with multiple pop-in events for the two mineral structures under $ScCO_2$ + brine treatment were observed. Numerous pop-in events occurred at indentation depths of less than 20 μm in granular structures and less than 30 μm in banded structures (Fig. 8). This suggests that the new pore structures induced by mineral dissolution primarily formed at these depths. Beyond these points, the pop-in events ceased and the force-displacement curves became continuous. The effects of mineral erosion on the two mineral structures diminished and eventually disappeared.

To further investigate the effects of different fluids on the indentation curves of each microstructure, the average and standard deviation of maximum indentation depth for each loading stage under various treatments were analyzed (Fig. 9). The maximum indentation depths for each loading stage in organic matrices under different fluid treatments were relatively consistent with the pre-treatment observations, along with their standard deviations (Fig. 9). In contrast, a notable discrepancy was observed in the maximum indentation depths of granular and banded structures, with the $ScCO_2$ + brine treatment showing the highest standard deviation, followed by the brine and $ScCO_2$ treatments. This indicates that $ScCO_2$-brine treatment exerted the most pronounced erosive effect on the two mineral structures. Notably, the differences in maximum depth between the organic matrix, untreated mineral structures, and mineral structures treated with $ScCO_2$ + brine were 20 and 30 μm for granular and banded structures, respectively. These values approximately approached the depths where pop-in events occur frequently (Fig. 8), suggesting that mineral erosion in the two structures under $ScCO_2$-brine treatment predominantly occurs up to coal surface depth of 20 and 30 μm under the fluid treatment conditions of this study.

It is worth noting that the erosion depths from the surface topography analysis using 3D laser scanning were generally smaller than those inferred from the indentation curve responses. This discrepancy may have arisen because deeper mineral erosion and minor structural damage are not directly detectable via 3D laser scanning. Nevertheless, both methods of erosion depth analysis indicate that banded structures

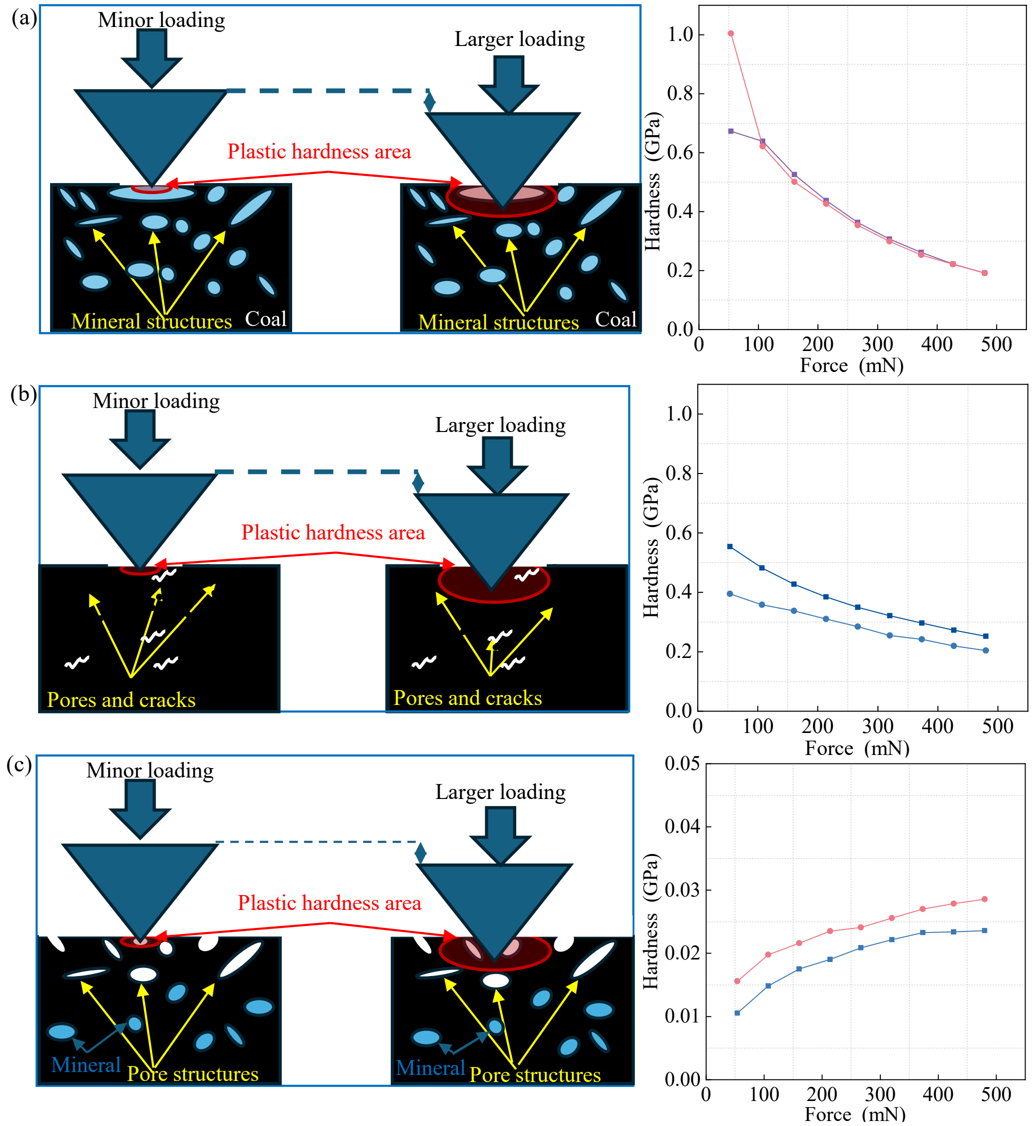

Fig. 10. Mechanism of hardness evolution due to structural and compositional heterogeneities. Hardness of (a) untreated mineral structures decreases with increasing force, (b) untreated organic matter decreases with increasing force and (c) mineral structures increases with increasing force under $ScCO_2$-Brine.

experienced the most severe erosion, followed by granular structures, under $ScCO_2$ + brine treatment. In contrast, mineral structures were only slightly affected under either $ScCO_2$ or brine treatment. The inherent homogeneity and chemical stability of organic matter largely preserve its surface topography, rendering it resistant to erosion.

4.2 Evolution of mechanical properties

4.2.1 Indentation size effect

As discussed in Section 3.2, the heterogeneity of mineral structures induces a scattered distribution of hardness and elastic modulus (Fig. 7). However, as the indentation depth increases, the mechanical parameters converged toward to a certain value (Manika and Maniks, 2006; Ebisu and Horibe, 2010; Han et al., 2015; Chua et al., 2019). ISE has been well-documented in numerous studies (Manika and Maniks, 2006; Ebisu and Horibe, 2010; Han et al., 2015; Chua et al., 2019). At the nanoscale, the size effect is often attributed to material deformation caused by intergranular dislocation slip (Mukhopadhyay and Paufler, 2006; Yang et al., 2020). At the micro-scale, the increase in indentation area reduces the impact of intergranular dislocation slip to a negligible level, where structural heterogeneity (including pre-existing and newly generated pore and fracture microstructures) and compositional heterogeneity (organic matter and minerals) within the indentation area are likely the primary contributing factors to ISE. This ISE is manifested as either a decrease or increase in hardness upon varying loading magnitudes for different fluid-treating conditions (Fig. 10) (Wang et al., 2024). As the loading force increases, the indenter gradually engages minerals, organic matter and pre-existing pores/fractures in mineral structures (Fig. 10(a)); organic matter and pre-existing pores/fractures in organic matrix (Fig. 10(b)); and newly formed pores/fractures and organic matter in newly formed pore structures (Fig. 10(c)). This results in a decrease in hardness (Figs. 10(a) and 10(b)) and an increase in hardness (Fig. 10(c)). Before $ScCO_2$-brine-coal interaction, the indentation area under a small load mainly focuses on the mineral structure. As the load increases, the indentation area gradually covers structures such as the organic matrix. This causes a gradual decrease in the mechanical properties of the mineral structure with increasing load. After the $ScCO_2$-brine-coal interaction, many minerals are eroded and dissolved, resulting in a loose coal skeleton. However, as the indentation depth increases, the indenter gradually comes into contact with the uneroded parts. The coal skeleton under the indentation area gradually transitions from loose to dense, leading to an increase in hardness as the load increases.

To minimize the influence of structural and compositional heterogeneities on the uniform mechanical properties of coal microstructures, the hardness values of the three coal microstructures were analyzed for indentation depths ranging from 5 to 20 μm. The results highlighting the ISE aid in selecting appropriate mechanical parameters from a specific loading stage to quantitatively evaluate changes in the mechanical properties of the coal microstructures under different fluid treatments (Fig. 11).

The hardness of the three coal microstructures under different fluid treatments demonstrated a noticeable size effect at indentation depths of 5-20 μm (Fig. 11). The function was selected for trend fitting based on the distinctive characteristics of the indentation experimental hardness test data, particularly the maximum indentation depth.

$$y = ax^b \tag{4}$$

It is evident that as erosion intensity increases, the fitted curve gradually flattens. To further analyze the variation trend of hardness with maximum indentation depth ($h_{\max}$) under the effect of different fluids, the tangent slope (S_t) and secant slope (S_c) of the fitted curve were used as indicators to determine the stability of hardness when the maximum indentation depth changes. The maximum indentation depth in the 5-20 μm interval was selected for calculation (Fig. 12).

Erosion caused by different fluids resulted in a decrease in S_t and S_c of the mineral structures, while those of the organic matrices remained stable (Fig. 12). The dissolution of mineral components induced by fluid treatment reduces compositional heterogeneity in the indenting area, thereby decreasing the fluctuation of mechanical parameters at different indentation depths and making the ISE less pronounced (Luo et al., 2020; Wang et al., 2022). This phenomenon coincides with the results that continuous multi-cyclic indentation experiments using SiO_2 crystals do not produce ISE (Li and Chen, 2009). However, due to pre-existing and newly generated pore structures, structural heterogeneity still influences the ISE until $h_{\max} \geq 12$ μm (Fig. 12). At this scale, the measured mechanical parameters should be considered as an effective value representing the mechanical properties of coal microstructures.

4.2.2 Quantitative characterization

Due to the heterogeneity of coal microstructures, their mechanical parameters varied across different loading stages during the indentation experiments. This variability introduces uncertainties in the quantitative characterization of the weakening effect under the $ScCO_2$-water-coal interaction. As discussed in Section 4.2.1, the effects of heterogeneity on the mechanical parameters decrease with increasing indentation depth, ultimately stabilizing at a value that represents the mechanical properties of the bulk microstructure. In our experiments, when the maximum indentation depth ($h_{\max}$) surpassed 12 μm, the ISE became negligible. After reviewing all the data (Fig. 7), it was found that only the last two loading stages met the requirements for all coal microstructures under different treatment conditions.

From the mechanical parameters of all microstructures under different fluid treatments from the first and the last two loading stages, it could be observed that the absolute values of H and E in the first cycle were significantly higher than those in the last two cycles, while the difference between the last two cycles was minimal (Fig. 13), consistent with the previous analysis (Fig. 12). Due to the ISE, the H and E values of the coal microstructure exhibited greater variability when the indentation depth was small. Only as the indentation depth increases can stable H and E values be used to accurately quantify the effect of fluid interactions on the mechanical properties of coal microstructure.

It could be observed that the mechanical parameters of the organic matrix after exposure to brine and $ScCO_2$ + brine fluids were slightly lower than those in the untreated state (Fig. 13). However, the overall difference was minor, indicating that the impact of these fluids on the organic matter component is limited. In contrast, all three fluids caused varying degrees of reduction in the mechanical parameters of the two mineral structures. The $ScCO_2$-brine fluid had the most pronounced effect (decreased 90% to 70%), followed by brine (decreased 60% to 40%), and $ScCO_2$ (decreased 20% to 30%) had the least impact. It should be noted that the mechanical parameters of organic matrices after $ScCO_2$ treatment are not discussed in detail due to equipment limitations and observation methods, which may not have fully captured the effects of 3D structural features on the indentation experiments.

In summary, the results of the 3D scanning experiments combined with the aforementioned analysis indicate that the three fluids exert a discernible erosive effect on the different microstructure areas of coal samples. The erosion effect on the organic matrices of coal samples is relatively weak, whereas the effect on the two mineral structures is more pronounced. On the one hand, $ScCO_2$-water-coal interaction can reduce the mechanical properties of mineral structures in fusinite by up to 90%; on the other hand, the increased porosity provides more space for CO_2 sequestration. Given that the primary component of coal is organic matter, it demonstrates stable properties under $ScCO_2$-water-coal interaction. Coal seams can maintain their integrity and stable mechanical properties while simultaneously increasing CO_2 storage capacity during the long-term sequestration of CO_2.

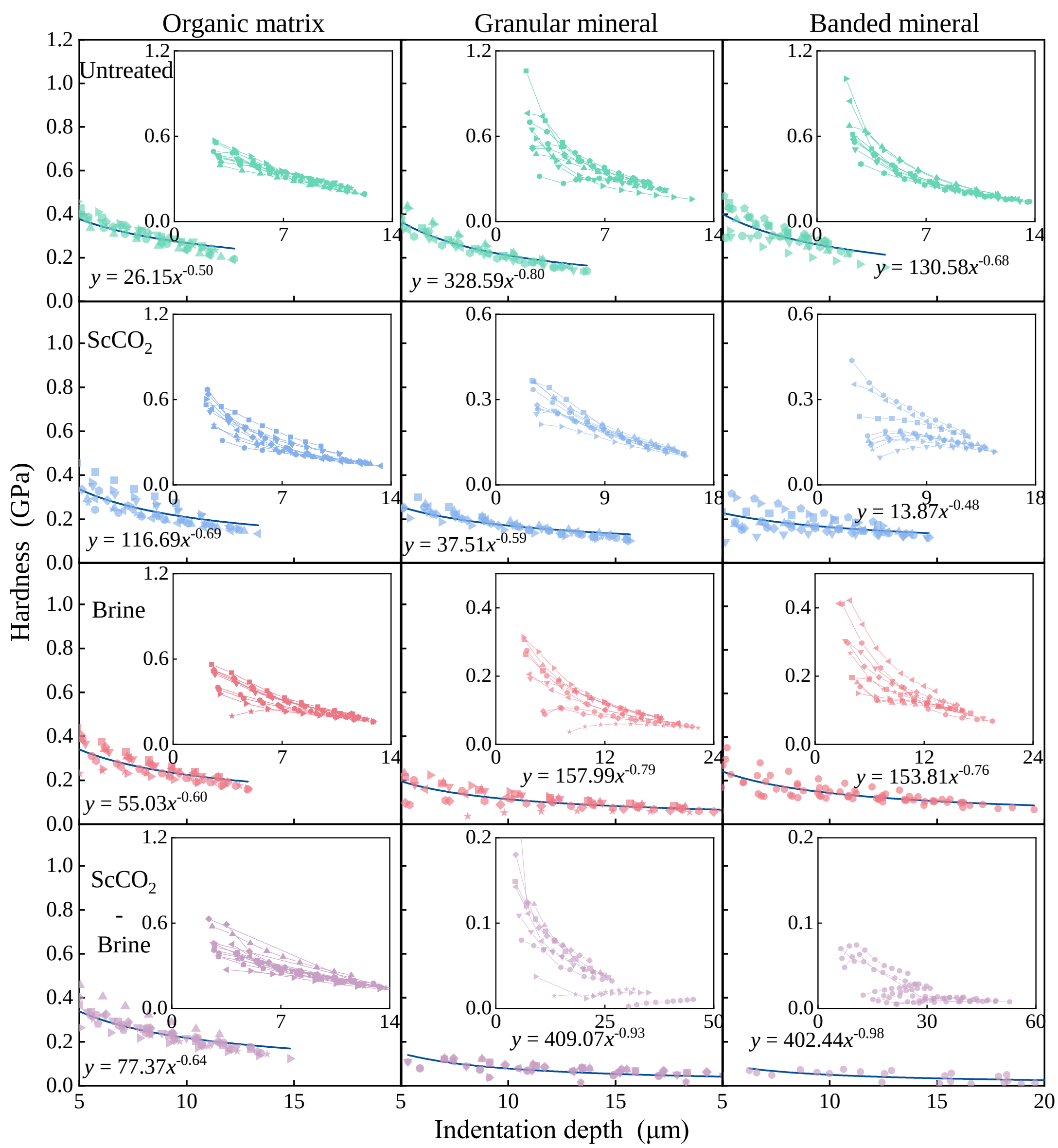

Fig. 11. Hardness versus maximum displacement (range of 5-20 μm) for each coal microstructure at different loading stages, before/after treatment with different fluids.

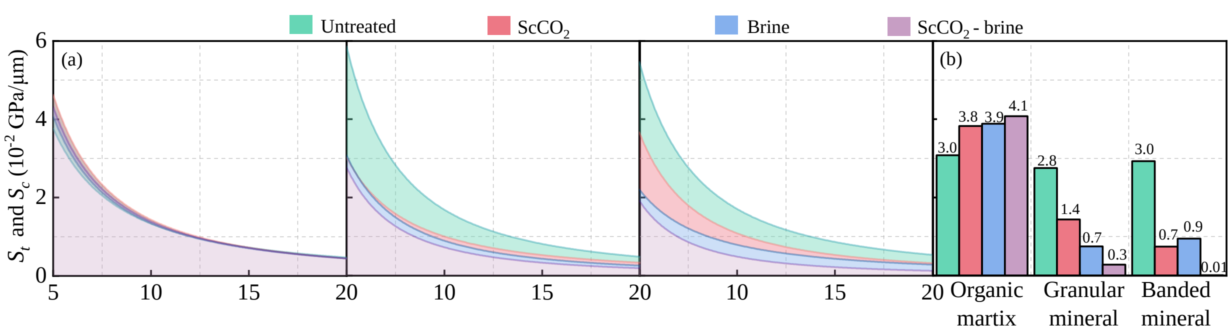

Fig. 12. Analysis of (a) S_t and (b) S_c of the fitted curves.

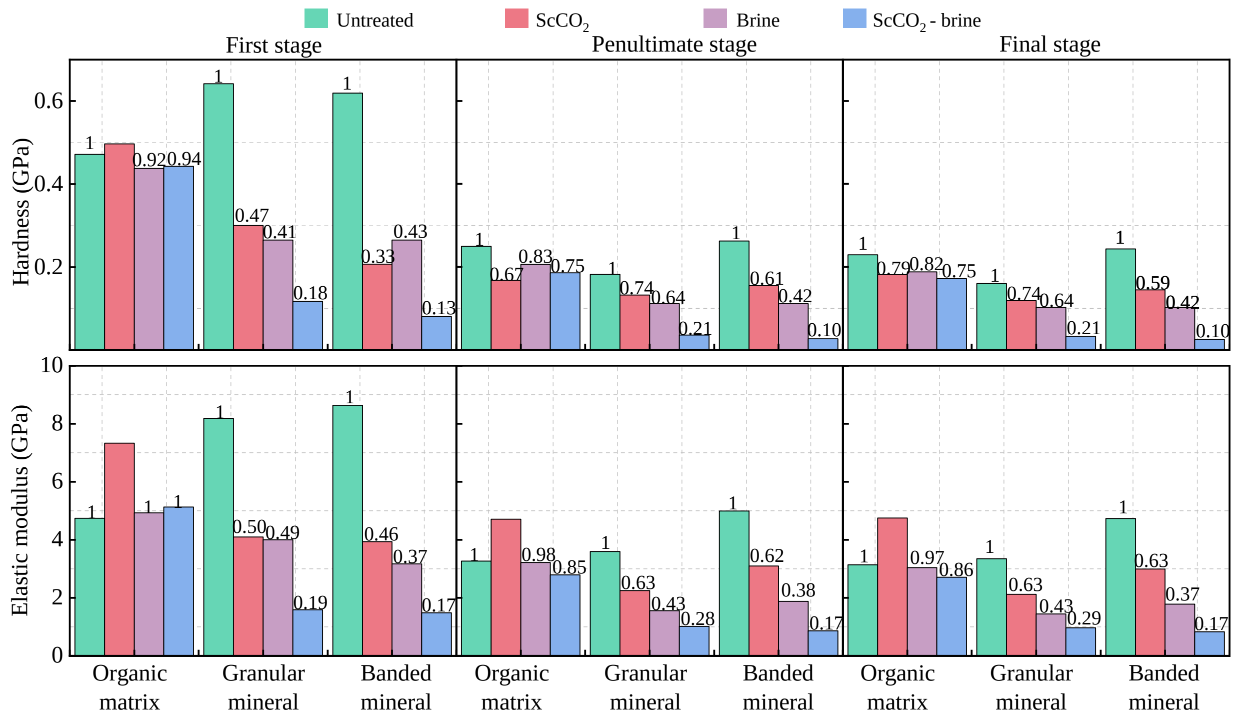

Fig. 13. Quantitative characterization of the mechanical property alterations under different fluid treatments at the last two loading stages.

5. Conclusions

Previous studies have primarily focused on the weakening of mechanical properties caused by $ScCO_2$-water-coal interaction, and they have lacked exploring the coal microstructural alterations and the underlying mechanisms of mechanical degradation. In this study, we investigated the changes in surface topology and mechanical parameters of coal microstructures under different fluid-soaking treatments using SEM, 3D laser scanning and indentation experiments, providing a quantitative framework to evaluate $ScCO_2$-water-coal interactions at the microscopic scale. The main conclusions drawn from this study are as follows:

1) The responses of coal microstructures to different fluid treatments were varied. Organic matrices demonstrated strong stability under all fluid treatments. Significant erosion, leading to newly formed pore structures, was observed in mineral structures under $ScCO_2$-brine treatment, with erosion depths reaching 1.6 μm in granular structures and 6.4 μm in banded structures. However, when exposed to $ScCO_2$ or brine alone, the erosion depths of the mineral structures remained negligible (within 0.5 μm).
2) The frequent pop-in events during indentation experiments confirmed severe damage to the mineral structures under $ScCO_2$-brine treatment. By employing indentation testing under various loading conditions, the effects of the ISE caused by structural and compositional heterogeneities can be evaluated, enabling the accurate quantitative analysis of changes in the mechanical properties of coal microstructures.
3) As the ISE decreased with increasing loading forces and indentation depth, the measured elastic modulus and hardness at the last two loading stages were found to represent the uniform the mechanical properties of coal microstructures. The results indicated that $ScCO_2$-water-coal interaction could reduce the H and E of coal microstructures by up to 90% in the indentation experiments.

Acknowledgements

This study was financially supported by the National Natural Science Foundation of China (Nos. 52204207, 52474209 and 52274111) and the Guizhou Provincial Major Scientific and Technological Program (No. [2024]029).

Supplementary file

https://doi.org/10.46690/ager.2025.09.04

Conflict of interest

The authors declare no competing interest.

References

Armitage, P. J., Faulkner, D. R., Worden, R. H. Caprock corrosion. Nature Geoscience, 2013, 6(2): 79-80.

Bashir, A., Ali, M., Patil, S., et al. Comprehensive review of CO_2 geological storage: Exploring principles, mechanisms, and prospects. Earth-Science Reviews, 2024, 249: 104672.

Chen, B., Harp, D. R., Zhang, Y., et al. Dynamic risk assessment for geologic CO_2 sequestration. Gondwana Research, 2023, 122: 232-242.

Chen, K., Liu, X., Nie, B., et al. Mineral dissolution and pore alteration of coal induced by interactions with supercritical CO_2. Energy, 2022, 248: 123627.

Chua, J., Zhang, R., Chaudhari, A., et al. High-temperature nanoindentation size effect in fluorite material. International Journal of Mechanical Sciences, 2019, 159: 459-466.

Deng, B., Nie, B., Liu, X., et al. Characteristics of the heterogeneous mechanical response of coal at the nano and micro-scale using instrumented indentation experiments. Chinese Journal of Theoretical and Applied Mechanics, 2022, 54(8): 2304-2317. (in Chinese)

Ebisu, T., Horibe, S. Analysis of the indentation size effect in brittle materials from nanoindentation load-displacement curve. Journal of the European Ceramic Society, 2010, 30(12): 2419-2426.

Fender, T. D., Rouainia, M., Van Der Land, C., et al. Geomechanical properties of coal macerals; measurements applicable to modelling swelling of coal seams during CO_2 sequestration. International Journal of Coal Geology, 2020, 228: 103528.

Friedlingstein, P., O'Sullivan, M., Jones, M. W., et al. Global carbon budget 2024. Earth System Science Data, 2025, 17(3): 965-1039.

Gathitu, B. B., Chen, W., McClure, M. Effects of coal interaction with supercritical CO_2: Physical structure. Industrial & Engineering Chemistry Research, 2009, 48(10): 5024-5034.

Han, Q., Chen, P., Ma, T. Influencing factor analysis of shale micro-indentation measurement. Journal of Natural Gas Science and Engineering, 2015, 27: 641-650.

He, H., Liu, P., Nie, B., et al. Micromechanical property evolution and damage mechanism of coal subjected to $ScCO_2$ treatment. Energy, 2024, 304: 132087.

Jiang, C., Xu, W., Deng, B., et al. Mineral erosion in different microstructures under $ScCO_2$-water-coal interactions: Implications for CO_2 sequestration in coalbeds. Energy & Fuels, 2025, 39(9): 4374-4394.

Jiang, R., Yu, H. Interaction between sequestered supercritical CO_2 and minerals in deep coal seams. International Journal of Coal Geology, 2019, 202: 1-13.

Joslin, D. L., Oliver, W. C. A new method for analyzing data from continuous depth-sensing microindentation tests. Journal of Materials Research, 1990, 5(1): 123-126.

Kossovich, E. L., Borodich, F. M., Epshtein, S. A., et al. Indentation of bituminous coals: Fracture, crushing and dust formation. Mechanics of Materials, 2020, 150: 103570.

Kossovich, E., Epshtein, S., Krasilova, V., et al. Effects of coals microscale structural features on their mechanical properties, propensity to crushing and fine dust formation. International Journal of Coal Science & Technology, 2023, 10(1): 20.

Li, M., Chen, W. Factors resulting in micron indentation hardness descending in indentation tests. Chinese Journal of Aeronautics, 2009, 22(1): 43-48.

Liu, T., Li, M., Li, J., et al. Interactions of CO_2-H_2O-coal and its impact on micro mechanical strength of coal. Geoenergy Science and Engineering, 2023a, 227: 211915.

Liu, A., Liu, S. Mechanical property alterations across coal matrix due to water-CO_2 treatments: A micro-to-nano scale experimental study. Energy, 2022, 248: 123575.

Liu, S., Sang, S., Ma, J., et al. Effects of supercritical CO_2 on micropores in bituminous and anthracite coal. Fuel, 2019, 242: 96-108.

Liu, B., Yao, J., Sun, T. Numerical analysis of water-alternating-CO_2 flooding for CO_2-EOR and storage projects in residual oil zones. International Journal of Coal Science & Technology, 2023b, 10(1): 73.

Luo, S., Lu, Y., Wu, Y., et al. Cross-scale characterization of the elasticity of shales: Statistical nanoindentation and data analytics. Journal of the Mechanics and Physics of Solids, 2020, 140: 103945.

Manika, I., Maniks, J. Size effects in micro- and nanoscale indentation. Acta Materialia, 2006, 54: 2049-2056.

Manjunath, G. L., Akono, A. T., Haljasmaa, I., et al. Role of CO_2 in geomechanical alteration of morrow sandstone across micro-meso scales. International Journal of Rock Mechanics and Mining Sciences, 2023, 163: 105311.

Masoudian, M. S., Airey, D. W., El-Zein, A. Experimental investigations on the effect of CO_2 on mechanics of coal. International Journal of Coal Geology, 2014, 128-129: 12-23.

Meng, M., Qiu, Z. Experiment study of mechanical properties and microstructures of bituminous coals influenced by supercritical carbon dioxide. Fuel, 2018, 219: 223-238.

Mouallem, J., Al-Abdrabalnabi, R., Raza, A., et al. Experimental investigation of CO_2 residual trapping in naturally water-wet and artificially tailored oil-wet limestones: Implications for geological CO_2 storage. Advances in Geo-Energy Research, 2025, 17(1): 43-55.

Mukhopadhyay, N. K., Paufler, P. Micro- and nanoindentation techniques for mechanical characterisation of materials. International Materials Reviews, 2006, 51(4): 209-245.

Nie, B., He, H., Liu, P., et al. Nanomechanical behavior of coal with heterogeneous minerals and pores using nanoindentation. Environmental Science and Pollution Research, 2024, 31(19): 28007-28024.

Niu, Q., Wang, X., Chang, J., et al. Influencing mechanisms of multi-scale pore-fracture responses of coals on their macro/micromechanical behaviors under $ScCO_2$ injection. Advances in Geo-Energy Research, 2024, 14(1): 64-80.

Perera, M. S. A., Ranjith, P. G., Viete, D. R. Effects of gaseous and super-critical carbon dioxide saturation on the mechanical properties of bituminous coal from the Southern Sydney Basin. Applied Energy, 2013, 110: 73-81.

Safaei-Farouji, M., Misch, D., Sachsenhofer, R. F., et al. CO_2 utilization and sequestration potential in deep coal seams: A case study on carboniferous coals from the karaganda basin, kazakhstan. Journal of CO_2 Utilization, 2025, 101: 103204.

Sampath, K. H. S. M., Perera, M. S. A., Ranjith, P. G., et al. CO_2 interaction induced mechanical characteristics alterations in coal: A review. International Journal of Coal Geology, 2019, 204: 113-129.

Shen, W., Ma, T., Zuo, L., et al. Advances and prospects of supercritical CO_2 for shale gas extraction and geological sequestration in gas shale reservoirs. Energy & Fuels, 2024, 38(2): 789-805.

Shi, F., Deng, B., Nie, B., et al. Deformation kinetics of coal-gas system during isothermal and dynamic non-isothermal processes. Gas Science and Engineering, 2023, 117: 205027.

Siqueira, T. A., Iglesias, R. S., Ketzer, J. M. Carbon dioxide injection in carbonate reservoirs – a review of CO_2-water-rock interaction studies. Greenhouse Gases: Science and Technology, 2017, 7(5): 802-816.

Su, E., Liang, Y., Chen, X., et al. Relationship between pore structure and mechanical properties of bituminous coal under sub-critical and super-critical CO_2 treatment. Energy, 2023, 280: 128155.

Sundal, A., Hellevang, H. Using reservoir geology and petrographic observations to improve CO_2 mineralization estimates: Examples from the Johansen formation, North Sea, Norway. Minerals, 2019, 9(11): 671.

Wang, P., Gao, Y., Wang, P. A comparative study of indentation size effect models for different materials. Scientific Reports, 2024, 14(1): 20010.

Wang, J., Yang, C., Liu, Y., et al. Using nanoindentation to characterize the mechanical and creep properties of shale: Load and loading strain rate effects. ACS Omega, 2022, 7(16): 14317-14331.

Wu, Q., Zhu, C. Enhancement of carbon sequestration capacity of coal through long-term geochemical reactions with $ScCO_2$-H_2O. Energy & Fuels, 2025, 39(32): 15400-15417.

Xu, S., Zhou, S., Zhou, J., et al. Multiscale pore structure evolution of Longmaxi shale induced by acid treatment. SPE Journal, 2022, 28(2): 831-844.

Yang, C., Xiong, Y., Wang, J., et al. Mechanical characterization of shale matrix minerals using phase-positioned nanoindentation and nano-dynamic mechanical analysis. International Journal of Coal Geology, 2020, 229: 103571.

Zagorščak, R., Thomas, H. R. Effects of subcritical and supercritical CO_2 sorption on deformation and failure of high-rank coals. International Journal of Coal Geology, 2018, 199: 113-123.

Zhang, L., Chen, L., Hu, R., et al. Subsurface multiphase reactive flow in geologic CO_2 storage: Key impact factors and characterization approaches. Advances in Geo-Energy Research, 2022a, 6(3): 179-180.

Zhang, F., Guo, H., Hu, D., et al. Characterization of the mechanical properties of a claystone by nano-indentation and homogenization. Acta Geotechnica, 2018, 13(6): 1395-1404.

Zhang, G., Ranjith, P. G., Lyu, Q. Direct evidence of CO_2 softening effects on coal using nanoindentation. Energy, 2022b, 254: 124221.

Zhang, C., Wang, Y., Kou, Z., et al. Recent research advances in enhanced CO_2 mineralization and geologic CO_2 storage. Advances in Geo-Energy Research, 2023, 10(3): 141-145.

Zhou, Z., Sheng, M., Ge, Z., et al. Mechanical properties and failure characteristics of supercritical carbon dioxide soak in water-bearing coal rocks. Energy, 2024, 286: 129599.